Structural changes in single-walled carbon nanotubes under non-hydrostatic pressures: x-ray and Raman studies

2003 New J. Phys. 5 143

(http://iopscience.iop.org/1367-2630/5/1/143)

New Journal of Physics
An Institute of Physics and Deutsche Physikalische Gesellschaft Journal

Structural changes in single-walled carbon nanotubes under non-hydrostatic pressures: x-ray and Raman studies

Sukanta Karmakar[1], Surinder M Sharma[1], P V Teredesai[2], D V S Muthu[2], A Govindaraj[3], S K Sikka[1,4] and A K Sood[2,3]

[1] Synchrotron Radiation Section, Bhabha Atomic Research Centre, Mumbai 400 085, India
[2] Department of Physics, Indian Institute of Science, Bangalore 560 012, India
[3] Chemistry and Physics of Materials Unit, Jawaharlal Nehru Centre for Advanced Scientific Research, Jakkur Campus, Jakkur, Bangalore 560 064, India
E-mail: asood@physics.iisc.ernet.in

New Journal of Physics **5** (2003) 143.1–143.11 (http://www.njp.org/)
Received 11 July 2003
Published 20 October 2003

Abstract. Using *in situ* x-ray diffraction and Raman scattering techniques, we have investigated the behaviour of single-walled carbon nanotubes bundles under non-hydrostatic pressures. It is seen that the diffraction line corresponding to the two-dimensional triangular lattice in the bundles is not reversible for pressures beyond 5 GPa, in sharp contrast to earlier results under hydrostatic pressure conditions. Most interestingly, radial breathing and tangential Raman modes of the pressure-cycled samples from 21 and 30 GPa match very well with those of the starting sample. Raman and x-ray results put together clearly suggest that the ordering of tubes in the bundles is only marginally regained with a very short coherence length on decompression.

[4] Present address: Scientific Secretary, Office of Principal Scientific Advisor to Government of India, Vigyan Bhavan Annexe, Maulana Azad Road, New Delhi 110 011, India.

Contents

1. Introduction

Single-walled carbon nanotubes (SWNTs), made of cylindrically rolled graphene sheets, have attracted a lot of attention due to their interesting and potentially useful electrical and mechanical properties. In particular, for mechanical properties, they have been hailed as the ultimate flexible springs of nature. While isolated tubes have been shown to retain their features even after bending by an angle of 120°, the bundles in which these tubes naturally grow, forming a triangular lattice, have also been shown to resist irreversible degradation to very high pressures. Under hydrostatic pressure conditions, the behaviour of the tubes has been studied by Raman scattering [1]–[9] as well as by x-ray diffraction [10, 11]. In Raman scattering, the radial breathing mode (RBM) has been shown to vanish at ∼2 GPa, recovering reversibly from decompression from ∼5 GPa in a few reports [2, 5, 9] as well as from a much higher pressure of 26 GPa in another study [4]. The loss of intensity of the RBM has been attributed to the loss of the Raman resonance condition [2] arising from the distortion of the tubes. Peters *et al* [5] have suggested that the deformation of the tubes from circular to oval shape makes the breathing mode not an eigen mode and hence not observable in Raman scattering above ∼2 GPa. The tangential modes (TM) continue to persist up to very high pressures (∼20 GPa) [4] and reappear on decompression from as high a pressure as 26 GPa. A change of slopes in the Raman frequencies of the TM with pressure have been observed at ∼2 GPa for carbon nanotubes with a diameter of ∼1.3 nm [5, 9]. These results have been attributed to flattening/polygonization of the nanotubes which are reversible when decompressed from a maximum pressure of ∼5 GPa. Molecular dynamics simulations [12] have shown that SWNT bundles collapse under hydrostatic pressure and the collapse pressure is inversely proportional to the diameter of the tubes: ∼2 GPa for $d = 1.3$ nm and ∼7 GPa for $d = 0.8$ nm. First principle calculations have also shown that the circular tubes collapse at ∼7 GPa to a phase with an elliptical cross-section [13]. X-ray diffraction studies have shown that while in some cases the translational order was lost at ∼2 GPa [11], in another study [10] it continued to persist to almost 9 GPa and the loss of translational order was preceded by a radial relaxation—a result consistent with the TM behaviour observed in Raman studies [4]. Interestingly, while the changes are found to be irreversible beyond a pressure of ∼5 GPa by Tang *et al* [11], the study of Sharma *et al* [10] clearly indicated that the reversibility is preserved up to a pressure of 13 GPa. However, both the studies give comparable values of bulk modulus of ∼34 GPa. The observed equation of state is found to be consistent with the first principles calculations [8].

The above discussion makes it clear that the behaviour of SWNTs under pressure has two issues: a structural transition at ∼2 GPa and reversibility/irreversibility of transformation at higher pressures. The results are varied in different studies, as also reviewed recently in a very comprehensive manner by Loa [14]. Theoretical studies [2, 5, 15] point out that the different

pressure behaviours may be related to the preponderance of different types of tube present in the sample. Generalized tight binding molecular dynamics calculations [2] of a (9, 9) nanotube bundle do not show any transition up to 5 GPa. On the other hand, a (10, 10) nanotube bundle is shown [5] to undergo a transition at 1.7 GPa. This can be related to the fact that the symmetry of the (10, 10) tube is incompatible with the triangular lattice, whereas (9, 9) tube symmetry is compatible. Similar conclusions are drawn from the density functional theory [15], wherein (10, 10) nanotubes show a pressure induced transformation, whereas (12, 12) tubes (whose symmetry is compatible with the triangular lattice) do not show any transition up to 6 GPa.

The behaviour of SWNTs has also been investigated under non-hydrostatic pressures. The first study, using a piston–cylinder method up to a pressure of ∼2.9 GPa, showed that the density of SWNTs increased rapidly to approach almost that of graphite and recovered completely on release of pressure [16]. The rapid compression was ascribed to reversible flattening and crushing of the tubes to an elliptical cross-section. Though the results are not explicitly shown, it was mentioned [16] that postmortem TEM and powder x-ray diffraction studies after 9 GPa pressure cycling revealed an irreversible transition from SWNT bundles to graphite. The neutron diffraction results on tubes of mean diameter 1.32 nm [17][5] under non-hydrostatic compression indicate that the tube cross-section deforms from circular to hexagonal, and this polygonization is complete at ∼5 GPa. The intensity of the (100) Bragg peak was found to be significantly reduced after releasing the pressure, indicating an irreversible deterioration of the bundle structure. A more recent study [18] suggests that when the SWNTs are subjected simultaneously to compression and shear deformation, SWNTs transform to a superhard form at ∼24 GPa, having bulk modulus comparable to that of diamond. This discussion clearly brings out that the pressure behaviour of the SWNT is still not well established. We have, therefore, carried out *in situ* x-ray diffraction and Raman studies under non-hydrostatic compression in a diamond anvil cell (DAC) and these results are reported here. One of the objectives of our study was to address the question of irreversibility of the transformation to graphite as reported in earlier reports [16]. Also, the non-hydrostatic study without the pressure transmitting fluid will also be free from the possible effects of the liquid medium on the inter-tube interactions.

2. Experimental details

SWNT bundles were prepared by the standard arc discharge method as explained in our earlier paper [4]. An analysis of the diffraction pattern at ambient conditions shows that SWNTs form a two-dimensional triangular lattice of lattice constant 17.97 Å. Taking the inter-tube gap as 3.12 Å [11], the mean diameter of the tubes is 1.49 nm which can correspond to (11, 11) armchair tubes and (19, 0) zigzag tubes or any other appropriate combination of integers n and m.[6] *In situ* high pressure angle dispersive x-ray diffraction studies were carried out at the Elettra Synchrotron Source with monochromatized x-rays ($\lambda = 1.0$ Å). The SWNT samples were loaded in a hole of ∼140 μm diameter drilled in a pre-indented (∼70 μm) steel gasket of a Mao–Bell type DAC without any pressure transmitting medium. For x-ray experiments, the gasket hole was filled by approximately half and then specks (∼5–10 μm size) of pressure marker (Au or Cu)

[5] Diamond cell configuration in the present experiment is closer to the V-configuration of this reference.

[6] For SWNTs the tube diameter d_t is related to integers (n, m) as $d_t = \mathbf{C_h}/\pi = \sqrt{3}a_{C-C}(m^2 + n^2 + mn)^{1/2}/\pi$, where a_{C-C} is the nearest-neighbour C–C distance (=1.42 Å) and $\mathbf{C_h}$ is the chiral vector $\mathbf{C_h} = n\mathbf{a}_1 + m\mathbf{a}_2$; $\mathbf{a}_1$, $\mathbf{a}_2$ being the primitive vectors of two-dimensional graphene sheet.

were loaded. More sample was then added and manually pressed till the gasket hole was fully filled. The diffraction patterns were recorded using an MAR345 image plate detector kept at a distance of ∼21 cm from the sample. Two-dimensional imaging plate records were transformed to one-dimensional diffraction profiles by the radial integration of diffraction rings using the software FIT2D. These experiments were repeated four times (first one up to 34 GPa, the second up to 1.6 GPa, the third up to 5.4 GPa and the fourth up to 30 GPa) [19].

Raman measurements were done under non-hydrostatic pressures up to 21 GPa using a double grating spectrometer (SPEX Ramalog5) equipped with a cooled RCA 31034 photo-multiplier tube and 514.5 nm line of argon ion laser. Confocal micro-Raman measurements were also carried out on the recovered pressure-cycled (PC) samples from the x-ray diffraction experiments (from 30 GPa), PC from Raman experiments up to a maximum pressure of 21 GPa as well as on the fresh samples of the same batch. These measurements were done using a DILOR-XY spectrophotometer equipped with a liquid nitrogen cooled CCD detector and 514.5 nm line from an argon ion laser. For Raman experiments, the pressure was measured by monitoring the ruby fluorescence R-lines. The ruby chip was placed on the top of the well packed SWNT sample in the gasket hole. Since pressure gradients are inevitable in a non-hydrostatic pressure environment, care was taken to perform Raman measurements on a spot very close to the small ruby chip.

3. Results and discussion

Bragg reflections at Q_{100} (∼0.402 Å^{-1}) scattering vector of the (100) planes represent the strongest feature for the two-dimensional triangular lattice of SWNT bundles as seen by the diffraction line at $2\theta \sim 4^\circ$ in figure 1 (lowest curve) which shows x-ray diffraction profiles at various pressures. It is seen that on increasing the pressure, the (100) diffraction line vanishes beyond 1.8 GPa. The diffraction pattern is regained when the pressure is released from 5.4 GPa. However, if the pressure is raised to 30 GPa, the (100) diffraction peak is not recovered on release of pressure within the time of our experiments (∼ a couple of hours). The observed loss of the two-dimensional long-range order at ∼2 GPa is in agreement with the results of the V-configuration of Rols *et al* [17] where this peaks vanishes ∼3 GPa. The difference in the pressure in our studies and that in [17] may be due to the better scattering cross-section of the neutron diffraction and also a slight difference in the scattering geometry. Figure 2 compares the pressure variation of the d-spacing of the triangular lattice under non-hydrostatic conditions (filled circles) with those from the earlier studies [10] under hydrostatic compression (open circles). Fitting the observed variation of the two-dimensional triangular lattice parameters with the one-dimensional Murnaghan equation [20] $a/a_0 = [(\beta'/\beta)P + 1]^{-1/\beta'}$, we obtain the linear bulk modulus $\beta = 20$ GPa and its pressure derivative $\beta' = 23$. Comparison of these values to those of SWNTs under hydrostatic pressures [10] ($\beta = 43$ GPa and $\beta' = 33$), we note that the triangular lattice is about twice as compressible than under the hydrostatic pressure condition. Although it is doubtful, the reason for this may be due to porosity in the sample under non-hydrostatic loading. In order to make comparison with the value of the bulk modulus obtained in piston–cylinder experiments, we need to know the compression along the tube axis. Taking the axial compression to be the same as in the graphitic plane with bulk modulus $\beta_a = 1250$ GPa [21], the volume bulk modulus B can be estimated as [22] $B^{-1} = 2\beta^{-1} + \beta_a^{-1}$, which gives $B = 10$ GPa. This value is very different from the value of 1 GPa obtained from the piston–cylinder method and 34 GPa under hydrostatic compression. This implies that the inherent compressibility of

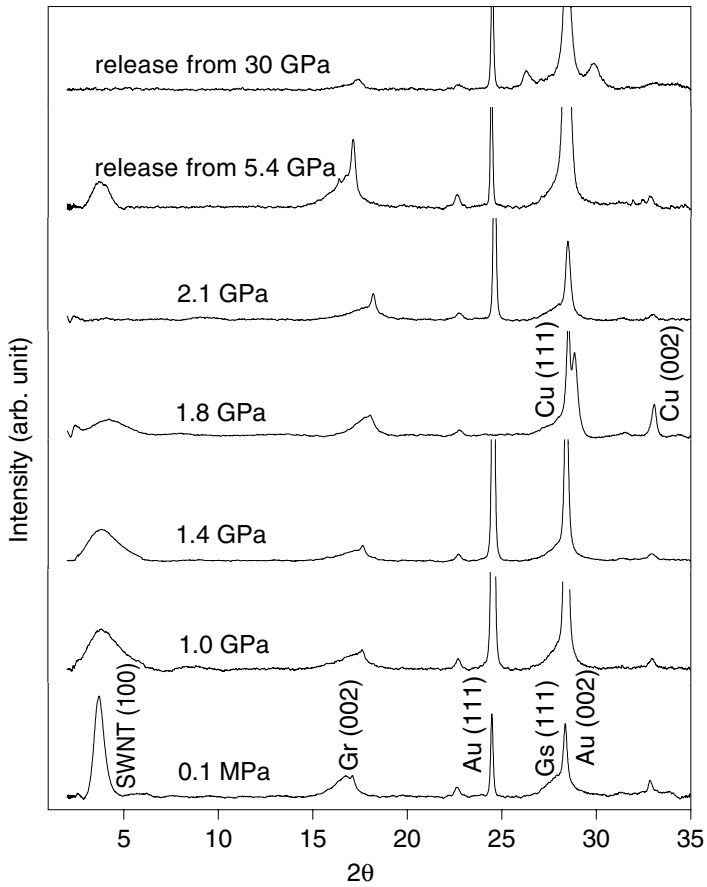

Figure 1. X-ray diffraction profile under various non-hydrostatic pressures. In the lowest panel, Gr and Gs refer to the diffraction lines from the graphite and the gasket material. The spectrum for 1.8 GPa was obtained in a different run using Cu as a pressure marker.

the tubes, as measured by the diffraction experiments, is far less than as monitored by the piston–cylinder method. This leads us to speculate that in piston–cylinder studies, in spite of reproducibility, there must be enough porosity around the bundle to lead to a much lower value of the bulk modulus.

Micro-Raman results for the samples recovered after the x-ray diffraction experiments, subjected to a maximum pressure of ∼30 GPa, are shown (filled circles) in figure 3 along with the Raman spectra of the starting sample (solid curve). Also shown in figure 3 are Raman spectra of PC samples from 21 GPa from high pressure Raman experiments (open circles) (to be discussed later). Micro-Raman experiments done on a couple of spots in the recovered samples are similar to the ones shown in figure 3. It is remarkable that both the radial breathing and TM as well as the disorder-related D-mode at ∼1350 cm^{-1} of the pressure quenched samples (from 21 GPa as well as from 30 GPa) agree remarkably well with those of the starting sample. Before we discuss the implications of these results, we present Raman results as a function of pressure (under non-hydrostatic condition) on the same batch of nanotubes. Figure 4 shows the RBM at a few pressures in an increasing pressure run. As in earlier reports [1]–[6] the intensity of the mode decreases rapidly with pressure and the mode cannot be observed beyond

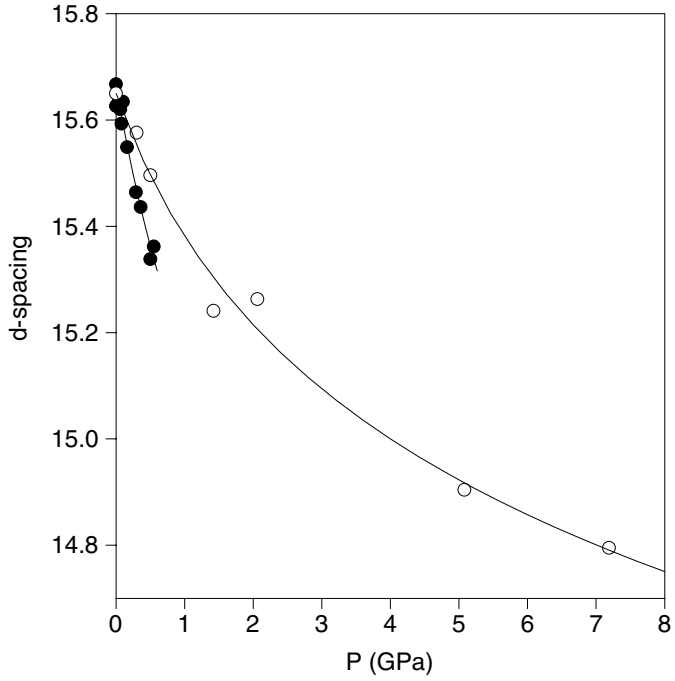

Figure 2. Variation of d-spacings under non-hydrostatic (filled circles) and hydrostatic (open circles) pressure conditions.

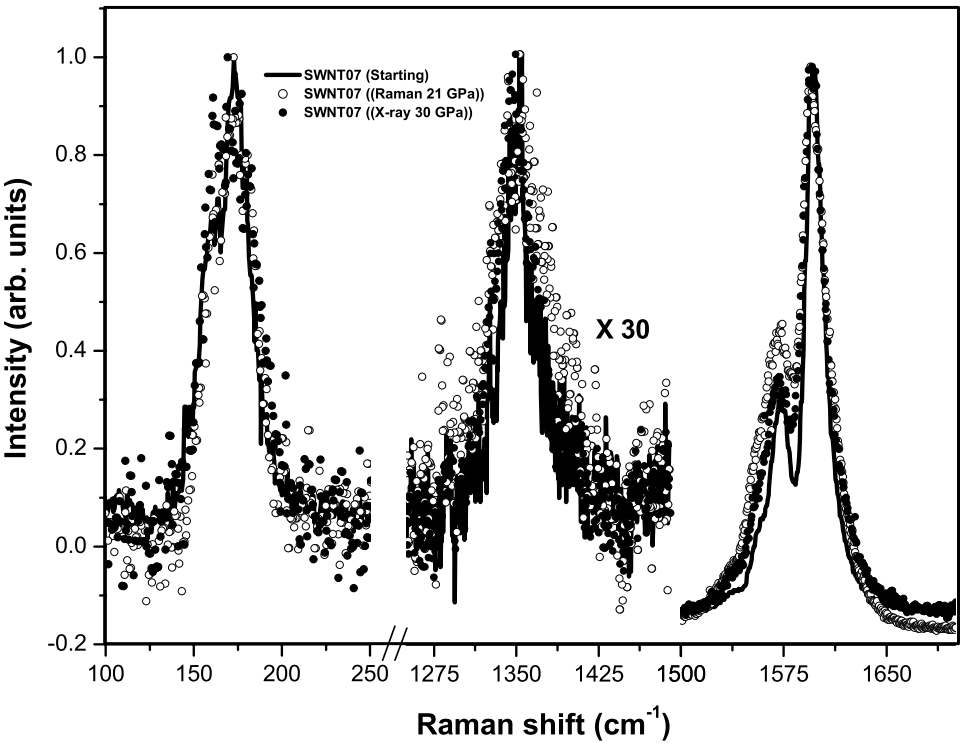

Figure 3. Raman spectra showing the RBMs, the disorder related D-mode and the TM of the starting sample (solid curve) and PC samples: filled circles, recovered from 30 GPa; open circles, recovered from 21 GPa.

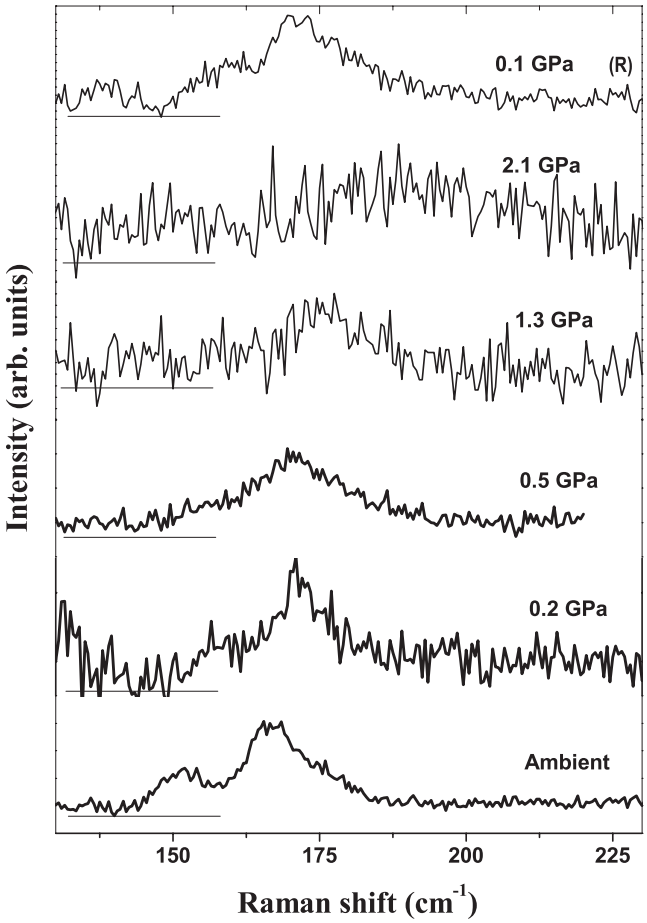

Figure 4. RBMs under various non-hydrostatic pressures. R denote the decreasing pressure runs in the top curve.

2 GPa. After gradually increasing the pressure to 21 GPa, the pressure is decreased and it is seen that the RBM is recovered at 1.8 GPa. Raman spectrum of the sample at 0.1 GPa in the decreasing pressure run (marked as R) is also shown in figure 4. Figure 5 shows the TM in both increasing and decreasing pressure runs. Here also, the intensities of the TM decrease and the linewidths increase with an increase in pressure. Raman spectra are discernable only up to ∼7 GPa. At ambient pressure, the spectrum can be decomposed into five Lorentzians, centred at 1533, 1554, 1570, 1595 and 1600 cm^{-1}. The pressure dependences of the strongest 1595 cm^{-1} mode (labelled as T_1) is shown in figure 6. A clear change in the pressure derivative ($d\omega/dP$) is seen at 2 GPa. The solid lines are linear fits with $d\omega/dP = 9.6 \pm 0.9$ cm^{-1} GPa^{-1} ($P < 2$ GPa) and 3.0 ± 0.3 cm^{-1} GPa^{-1} ($P > 2$ GPa). The change in slope in the present Raman experiments at ∼2 GPa is similar to the one observed under the hydrostatic pressure condition [5, 9], which has been attributed to the flattening [5] or collapse [9] of the nanotubes. It can be clearly seen that the value of the slope in the low pressure range for non-hydrostatic pressures is higher than its value of 5.3 cm^{-1} GPa^{-1} under hydrostatic pressures [4]. Recalling that the Gruneisen parameter of a mode is $\gamma_i = (B/\omega_i)\, d\omega_i/dP$, this can be readily understood from the fact that the bulk modulus (non-hydrostatic) is about half of its value under hydrostatic pressure conditions. It may be noted that our earlier results on hydrostatic pressure did not show

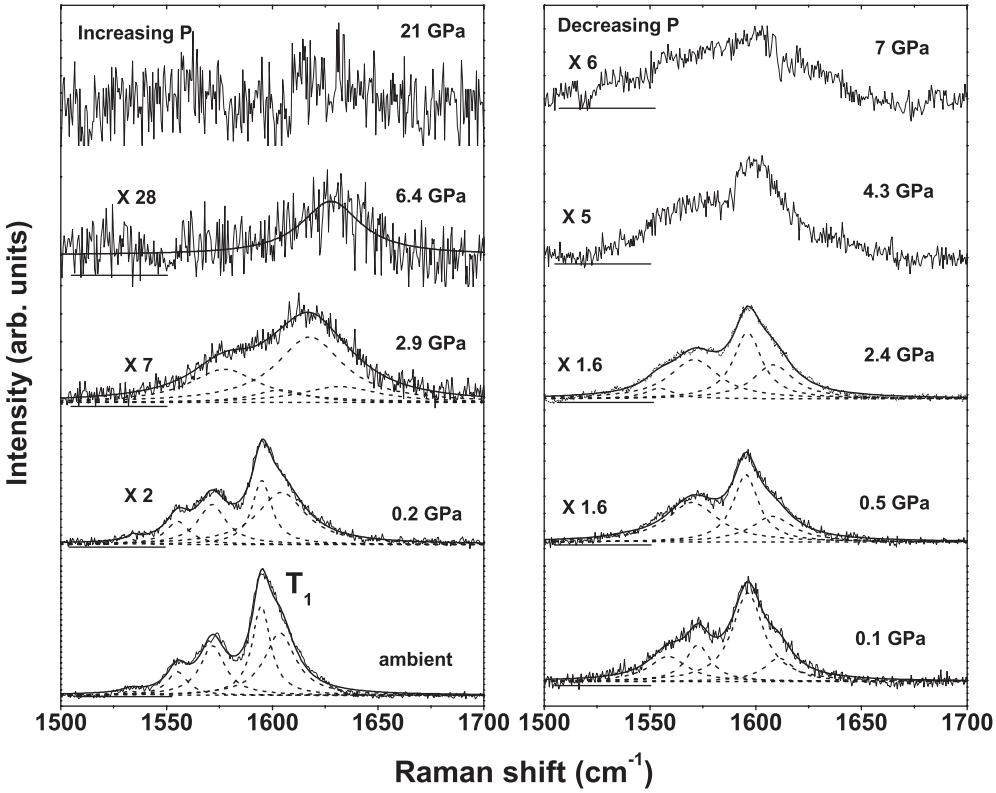

Figure 5. TM of SWNTs under non-hydrostatic pressures in increasing and decreasing pressure runs. The thick smooth solid curves represent the resultant fit to a sum of Lorentzians shown by dashed curves.

the 2 GPa transition. This may be because the samples used in the earlier study (tube diameter) and the present study are different.

The vanishing of the TM at much lower pressures than under hydrostatic pressures [4] indicates, as expected, a much higher degree of deformation. Several workers have investigated the nature of structural deformations in the tubes. The role of faceting or polygonization has been well investigated [2, 11], [23]–[25] in the context of compressibility as well as possible deformations such as buckling. In particular, an elastic honeycomb model predicts [24] that for tubes of diameter ∼1.3 nm, the tubes buckle at ∼1.8 GPa. However, such a model would not explain a systematic loss of translational coherence[7], as indicated by reducing diffracted intensity (corresponding to Q_{100}) as well as the intensity of RBMs. Chesnokov *et al* [16] and Peters *et al* [5] have also suggested a change in cross-section of tubes to oval or elliptical shape in contrast with the polygonization. In this context we should also note that not all the tubes (such as (5, 0) and (7, 0)) are favourably predisposed to polygonization [26]. Our computed diffraction patterns of the crystalline bundle show that the polygonization or faceting does not reduce the diffracted intensity for the (100) peak. However, changing to an elliptical shape systematically lowers the diffracted intensity as the ratio of major and minor axis increases, and by the time the ratio

[7] Coherence length as evaluated using FWHM of (100) peak and Scherrer's formula show that it almost decreases linearly from 90 Å at ambient pressure to 10 Å at ∼1.8 GPa.

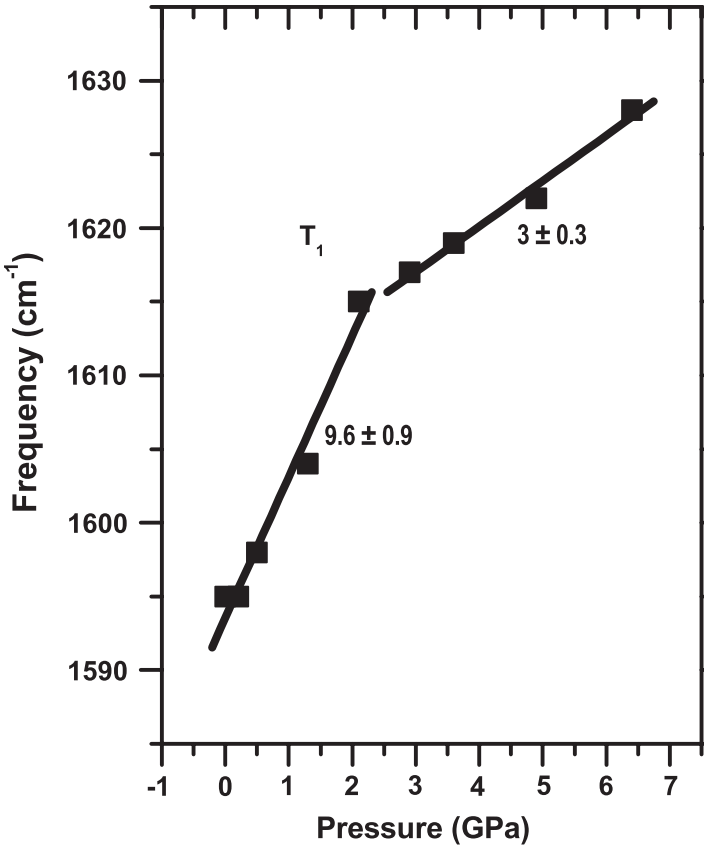

Figure 6. Pressure dependence of the frequency of the TM T_1. The lines are the linear fits with slopes indicated next to them.

becomes ∼2 the diffracted intensity of the (100) peak is only comparable to that of the $(1\bar{1}0)$ peak[8], which is practically unobservable in the present case. These calculations suggest the need for experiments with purer tubes having lower overall background to help settle questions regarding deformation.

We now come to the issue of reversibility of pressure-induced deformations. X-ray data show that the (100) diffraction line is not recovered on decompression from 30 GPa (figure 1). However, the Raman spectra associated with the radial breathing and TM of this PC sample agree very well with those of the starting (S) sample. To make it clear, PC refers to the sample

[8] X-ray diffraction patterns are computed by Powdcell software. Starting with the triangular array of (11, 11) circular tubes, diffraction patterns of SWNT bundles are generated with various elliptic deformations (varying the eccentricity of the tubes). To retain the perimeter fixed (as the C–C bond distance hardly changes at such low pressures), the tubes can be deformed elliptically only in a particular way (particular combinations of a and b), specific to the tube diameter. Also to retain the close packing of the tubules, the triangular lattice deforms into an oblique shape. In the new structure, atom coordinates are generated with respect to the new oblique axes and the diffraction patterns are generated accordingly. The computed diffraction pattern shows that as the tubes deforms elliptically, the two-dimensional triangular lattice structure vanishes and the (100) peak intensity goes down. Starting with triangular array of circular tubes (of diameter 14.92 Å) we find that as the tubes become elliptic (with major and minor axes becoming 19 Å and 9 Å respectively), the (100) peak intensity becomes comparable with that of the $(1\bar{1}0)$ peak which is unobservable in the present experiment.

recovered from the DAC after subjecting it to the maximum pressure in that run. A similarity of the TM implies that the tube structure of the PC sample is the same as the starting sample. Most interesting is the observation that the RBMs are the same for the PC and starting samples, allowing us to make the following inferences.

(i) On decompression, the cross-section of the tubes should revert to the circular shape, as in the starting sample because the RBM is still an eigen mode.

(ii) The frequency of the RBM in a bundle is about $\sim$12 to 14 cm^{-1} higher than that of the isolated tube.

This implies that the nanotubes in the PC sample are still in the form of bundles. We suggest that this can be reconciled with the non-observation of the (100) diffraction line in the PC sample if the size of bundles in the PC sample is very small which will have a very short coherence length, not allowing the (100) diffraction line to be seen in x-ray, but sufficient to influence the RBM. Each tube in a bundle of three tubes will have two nearest neighbours and the central tube in a bundle of seven tubes will have six nearest neighbours; each tube at the periphery will have three. Such small bundles will not show the (100) diffraction line, but will have the RBM as in a bigger bundle.

To conclude, our studies confirm the inherent mechanical resilience of the SWNTs. The essential tubular nature is retained on decompression even from 30 GPa. However, x-ray and Raman data on the PC samples from 30 GPa suggest that the translation order in the triangular lattice in the bundle is irreversibly reduced, perhaps to only the nearest-neighbour distance in the triangular lattice. It will be interesting to perform transmission electron microscopy of the PC samples to directly quantify the reduced size of the bundles.

Acknowledgments

The x-ray diffraction experiments were performed on the x-ray diffraction beamline of Synchrotron Source Elettra, Italy under Proposal no 2001047. We thank the Department of Science and Technology for financial assistance and Professor C N R Rao for the samples of SWNTs and his continued interest.

References

[1] Sood A K, Teredesai P V, Muthu D V S, Sen R, Govindaraj A and Rao C N R 1999 *Phys. Status Solidi* b **215** 393

[2] Venkateswaran U D, Rao A M, Richter E, Menon M, Richter A, Smalley R E and Eklund P C 1999 *Phys. Rev.* B **59** 10928

[3] Thomsen C, Reich S, Goni A R, Jantoljak H, Rafailov P M, Loa I, Syassen K, Journet C and Bernier P 1999 *Phys. Status Solidi* b **215** 435

[4] Teredesai P V, Sood A K, Muthu D V S, Sen R, Govindaraj A and Rao C N R 2000 *Chem. Phys. Lett.* **319** 296

[5] Peters M J, McNeil L E, Lu J P and Kahn D 2000 *Phys. Rev.* B **61** 5989

[6] Reich S, Jantoljak H and Thomsen C 2000 *Phys. Rev.* B **61** 13389

[7] Teredesai P V, Sood A K, Sharma S M, Karmakar S, Sikka S K, Govindaraj A and Rao C N R 2001 *Phys. Status Solidi* b **223** 479

[8] Reich S, Thomson C and Ordejon P 2002 *Phys. Rev.* B **65** 153407

[9] Sandler J, Shaffer M S P, Windle A, Halsall M P, Montes-Moran M A, Cooper C A and Young R J 2003 *Phys. Rev.* B **67** 035417
[10] Sharma S M, Karmakar S, Sikka S K, Teredesai P V, Sood A K, Govindaraj A and Rao C N R 2001 *Phys. Rev.* B **63** 205417
[11] Tang J, Qin L C, Saski T, Yudasaka M, Matsushita A and Iijima S 2000 *Phys. Rev. Lett.* **85** 1887
[12] Elliott J A, Sandler J K W, Young R J, Windle A H and Shaffer M S P 2003 unpublished
[13] Reich S, Thomsen C and Ordejon P 2003 *Phys. Status Solidi* b **235** 354
[14] Loa I 2003 *J. Raman Spectrosc.* **34** 611
[15] Sluiter M H F, Kumar V and Kawazoe Y 2002 *Phys. Rev.* B **65** 161402
[16] Chesnokov S A, Nalimova V A, Rinzler A G, Smalley R E and Fischer J E 1999 *Phys. Rev. Lett.* **82** 343
[17] Rols S, Gontcharenko I N, Almirac R, Sauvajol J L and Mirebeau I 2001 *Phys. Rev.* B **64** 1534011
[18] Popov M, Kyotani M, Nemanich R J and Koga Y 2002 *Phys. Rev.* B **65** 033408
[19] Heinz D L and Jeenloz R 1984 *J. Appl. Phys.* **55** 885
[20] Murnaghan F D 1944 *Proc. Natl Acad. Sci. USA* **30** 244
[21] Hanfland M, Beister H and Syassen K 1989 *Phys. Rev.* B **39** 12598
[22] Fei Y and Mao H 1993 *J. Geophys. Res.* **98** 11875
[23] Yakobson B I, Brabec C J and Bernholc J 1996 *Phys. Rev. Lett.* **76** 2511
[24] Tersoff J and Ruoff R S 1994 *Phys. Rev. Lett.* **73** 676
[25] Ru C Q 2000 *Phys. Rev.* B **62** 10405
[26] Yildirim T, Gulseren O, Kilic C and Ciraci S 2000 *Phys. Rev.* B **62** 12648